Modeling ultrashort laser-induced emission from a negatively biased metal

W. Wendelen,[1,a)] B. Y. Mueller,[2,b)] D. Autrique,[1,2] A. Bogaerts,[1] and B. Rethfeld[2]
[1]*Research Group PLASMANT, University of Antwerp, Universiteitsplein 1, 2610 Wilrijk, Belgium*
[2]*Department of Physics and Research Center OPTIMAS, University of Kaiserslautern, Erwin-Schrödinger-Straße 46, 67663 Kaiserslautern, Germany*

(Received 15 July 2013; accepted 16 October 2013; published online 26 November 2013)

A theoretical study of ultrashort laser-induced electron emission from a negatively biased metallic cathode has been performed. Classical as well as tunneling electron emission mechanisms are considered. It was found that electron emission is governed by an interplay of processes inside as well as above the cathode. A hybrid model is proposed, where the electron distribution within the target is retrieved from Boltzmann scattering integrals, while the charge distribution above it is studied by a Particle-In-Cell simulation. The results indicate that non-equilibrium effects determine the initial emission process, whereas the space charge above the target suppresses the effectively emitted charge. © *2013 AIP Publishing LLC*. [http://dx.doi.org/10.1063/1.4830378]

Electron emission induced by an ultrashort laser pulse is encountered in many applications, among which the production of ultrashort electron bunches and the study of ultrafast time-resolved phenomena.[1–10] Furthermore, electron emission can have a big influence on processes in several applications involving ultrashort laser pulses interacting with solids.[11–15] The mechanisms of laser induced electron emission have been studied for a long time,[8,16–20] but despite the widespread use of the phenomenon, there is no theory that adequately combines all the underlying processes. For instance, the electron distribution, charge transport, and carrier dynamics within the target,[12,21–23] as well as surface effects[24–27] and the evolution of the charge density above the target,[23,28–32] have been discussed intensively. All these processes influence each other, and have a considerable effect on the emitted charge. In particular, the space charge, created by the emitted electrons accumulating above the target surface, reduces electron emission substantially.[23,28,30] A negative bias to the emitter has been a commonly adopted method to overcome this space charge effect.[27,28,33–39] The resulting electric field counteracts the potential barrier formed by the work function, which can induce field emission field emission of tunneling electrons.[40] While field emission without laser excitation is commonly described by the Fowler-Nordheim equation,[16] an approach for the non-equilibrium electron distribution is necessary to describe ultrashort laser induced electron emission.[23,41,42] In this paper, a hybrid model for ultrashort laser-induced electron emission is proposed, which takes into account the non-equilibrium distribution within the target and the space charge effect above the target. The non-equilibrium distribution is calculated by solving the Boltzmann equation, while the space charge effect is evaluated by a Particle-In-Cell (PIC) model.

Field emission is mainly determined by the shape of the potential barrier $V(z)$ through which the electrons tunnel.[40] In the present work, we consider a time-dependent electrostatic potential defined by three terms

$$V(t,z) = \phi - eE_{\text{ext}}z + V_{\text{sc}}[\rho(t,z)]. \tag{1}$$

The work function ϕ and the external electric field E_{ext} form initially a triangular shape. In addition to these two contributions, the space charge, created by the emitted electrons, is described by the term $V_{\text{sc}}[\rho(t,z)]$, which is determined by the time dependent charge distribution $\rho(t,z)$ above the target surface. Generally, Eq. (1) should be extended with an appropriate surface potential, as the emitted electrons induce a net positive charge in the target. Hence in this work, a step-like potential at the surface is implemented, which has been shown to hold for conditions similar to those discussed in the present model.[26] A schematic representation of the transient potential barrier is given in Fig. 1.

We have studied electron emission from gold, assuming three different external electric fields ($E_{\text{ext}} = 10^7$ V/m, 10^8 V/m and 10^9 V/m), for a 100 fs square laser pulse and a wavelength of 800 nm. The metal samples are treated as

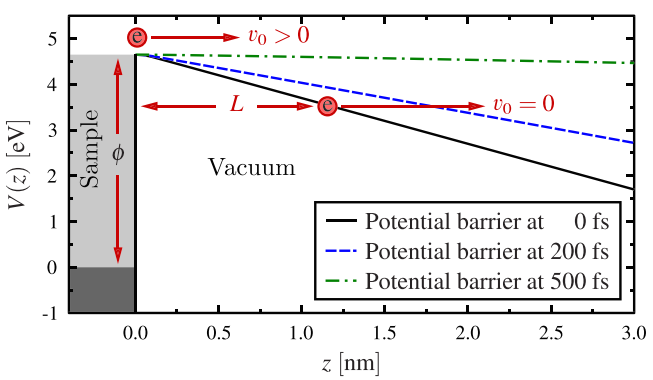

FIG. 1. The time-dependent potential barrier $V(t,z)$ at three different times. The curves are calculated by Eq. (1) with the time-dependent charge distribution obtained from our hybrid model after an excitation with a 100 fs laser pulse with an absorbed fluence of 5.31 J/m^2 and an external field of 10^9 V/m. The potential energy is defined with respect to the Fermi energy. L and v_0 denote the tunneling distance and the initial velocity of the emitted particle.

[a)]Electronic mail: wouter.wendelen@uantwerpen.be
[b)]Electronic mail: bmueller@physik.uni-kl.de

perfectly homogeneous and isotropic media. The laser excitation and thermalization of the electrons as well as the energy transfer to the lattice within the sample, are evaluated by Boltzmann scattering integrals.[43,44,48] With the electron distribution $f(k)$, the electron emission flux J_z can be determined by[23]

$$J_z = \int_0^\infty dk_z\, j(k_z) \tag{2a}$$

$$j(k_z) = \frac{e\hbar}{4\pi^2 m}\int_0^\infty dk_r\, f(k) k_z k_r W(k_z). \tag{2b}$$

Here, k_r, k_z are the momentum parallel (r) and perpendicular (z) to the surface, respectively, whereas $j(k_z)$ denotes the differential emission flux. For a given potential barrier $V(z)$, the electron escape probability W is given by[40]

$$W(\varepsilon_z, V) = \left|\exp\left(-\sqrt{\frac{2m}{\hbar^2}}\int_0^L dz\sqrt{V(z)-\varepsilon_z}\right)\right|^2, \tag{3}$$

where the energy $\varepsilon_z \equiv \varepsilon(k_z)$ is calculated from the dispersion relation.[44] Equation (3) expresses the probability for an electron of energy ε_z to tunnel through a potential barrier $V(z)$ of length L. When ε_z exceeds the work function, the electron escape probability is set to unity. In this case, the electron can be emitted in the classical way. Hence, Eq. (2) contains contributions from tunneling electrons generated by laser induced field emission ($\varepsilon_z < \phi$), as well as the common thermionic and multiphoton emission mechanisms ($\varepsilon_z > \phi$). During ultrashort laser excitation, the electrons are driven out of equilibrium and steps around the Fermi level are observed in the electron distribution:[43,44] Electrons below the Fermi energy absorb photons and the electron occupation number at higher energies gradually increases. In the end, a high energy step in the distribution function, larger than the equilibrium thermalized tail, will be observed.[23,43,44] In Fig. 2, the difference between the differential emission flux under non-equilibrium conditions and its corresponding equilibrium value is shown.[23,44] The latter has been determined from a Fermi distribution defined by the same internal energy and electron density as in the corresponding non-equilibrium distribution function.[44,47] Note that field emission under equilibrium conditions underestimates electron emission considerably. After some hundreds of femtoseconds, the distribution thermalizes and the non-equilibrium and equilibrium distributions coincide (see Fig. 2). However, the main contribution to the emitted charge is delivered at the initial emission stage during laser excitation ($t \lesssim 100$ fs). Hence, it is essential that the non-equilibrium electron distribution is considered for calculations of electron emission after an ultrafast laser excitation. Fig. 2 considers a hypothetical case without any space charge effects. These will now be taken into account by a PIC-model.[23,28,30,45] Here, electrons are treated as macroparticles with a certain weight, which move through a one dimensional (1D) grid, ranging from the metal surface to a certain cutoff distance, with a velocity according to the local electric field. The weight of each particle is given by the amount of electrons it represents, and is calculated by integrating $j(k_z)$ over defined time- and k_z-intervals. These intervals define the initial position and velocity of the macroparticle in the PIC-grid as follows: The particles with energy above the work function leave the surface with a velocity derived from the corresponding electron dispersion relation.[23,44] The tunneling particles with energy below the work function start at rest. Their initial position corresponds to the end of the potential barrier they are tunneling through, i.e., at the distance L where the electrostatic potential equals the electron energy inside the metal. An example for this length L entering Eq. (3) is illustrated in Fig. 1. Finally, electrons which reach a certain cutoff distance are considered as effectively emitted. This cutoff distance Z_{cutoff} is taken as 100 nm, which is small enough to ensure a 1D situation, and large enough to capture the space charge effect.

In Fig. 3, the influence of the space charge effect on the differential emission flux is shown. When the space charge is included, the emission drops considerably over time for

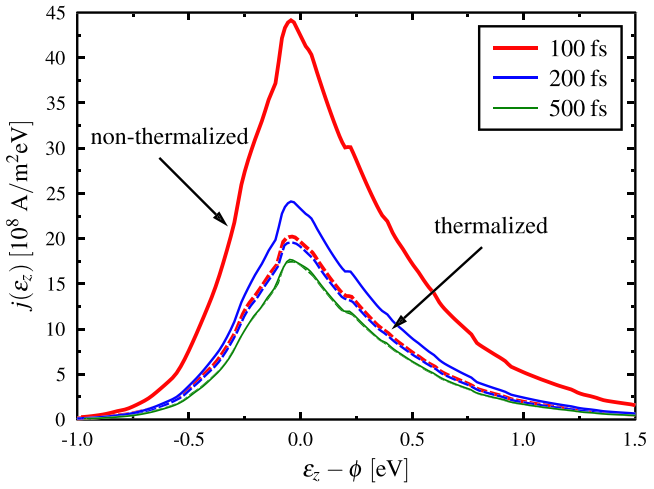

FIG. 2. The differential emission flux $j(\varepsilon_z)$, taken at three different times for a thermal electron distribution (dashed) and a non-equilibrium distribution (solid). The absorbed laser fluence was taken as 2.99 J/m^2 and the external electric field is 10^9 V/m. Note that the space charge effect is not included yet.

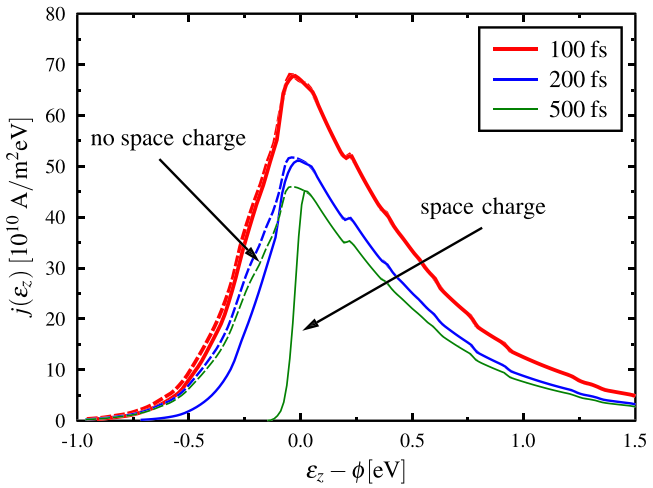

FIG. 3. The differential emission flux $j(\varepsilon_z)$, taken at three different times for emission with (solid) and without (dashed) the space charge correction, respectively. The absorbed laser fluence is 5.31 J/m^2 and the external electric field is 10^9 V/m.

energies below the work function. As can be seen in Fig. 1, the space charge effect broadens the potential barrier, and the electron tunneling probability decreases substantially for electrons below the work function, see Eq. (3). This effect is most visible after several hundreds of femtoseconds, when more charge has accumulated above the target surface. As a reference, results are shown for a potential barrier without space charge correction, i.e., $V_{sc} = 0$ in Eq. (1). Since in this case, the barrier is independent of the charge distribution above the surface, there is no decrease in electron escape probability, and emission by tunneling electrons continues. For Fig. 3, a high fluence was assumed since the space charge effect is most influential for large emission fluxes. In the simulations of Fig. 2, lower fluences were applied since at high fluences thermalization occurs faster.[23,44] In this work, the laser fluences should be considered as absorbed ones, coupled directly to the target after reflection.

Another consequence of the space charge effect is shown in Fig. 4. Since the space charge correction V_{sc} (see Eq. (1)) counteracts the external electric field, it is possible that enough charge accumulates above the surface to neutralize E_{ext} at Z_{cutoff}. As a result, the uniform electric field caused by the planar charge will compensate the external electric field. Hence, this critical amount of charge Q_{crit} is determined by

$$Q_{crit} = \epsilon_0 E_{ext}. \tag{4}$$

Evidently, Q_{crit} only depends on the external electric field. In Fig. 4, it can be seen that the amount of emitted charge rises in relation with the laser fluence until Q_{crit} has been reached. Afterwards, saturation is observed. Once the external electric field has been neutralized, the negative charge above the target pushes electrons back. Hence, the amount of effectively emitted charge is reduced substantially. Similar behavior has been observed in experiments, and attributed to the space charge effect.[46] For comparison, the emitted charge without the influence of the space charge effect is also shown in Fig. 4.

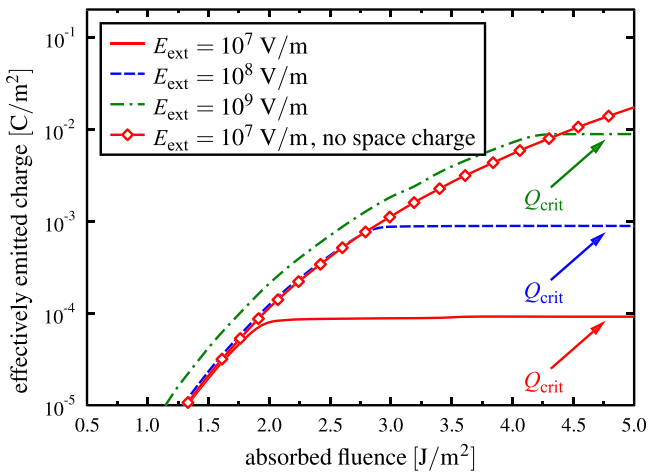

FIG. 4. The amount of effectively emitted charge after 2 ps for three different external fields in dependence on the absorbed laser fluence. The emitted charge without the influence of the space charge is also shown for $E_{ext} = 10^7$ V/m.

In short, the results show that the present model incorporates the influence of the non-equilibrium distribution and the space charge correction. Note that in several works, a constant, specific image charge correction term in Eq. (1) was used, while the space charge effect was neglected.[8,40–42] The correction term was derived for one point charge near a conductor and assumed a steady situation. Since in a one dimensional model the charges should be treated as charged infinite parallel planes and because the image charge correction should reflect the dynamic nature of the emission process, its use was found to be incompatible with the problem under study. In our work, image charge effects are implemented through the boundary conditions of the electric field, and a step potential is adopted at the surface. In their previous work, Faraggi *et al.*[26] found that this provides a reasonable description of laser-induced electron emission from metallic targets. Nevertheless, it should be noted that an alternative approach could be followed for the description of the surface potential. Here, the time dependent Schrödinger equation (TDSE) could provide such an alternative. The TDSE allows an adequate description of the surface potential states.[24–26] Moreover, it can be combined with the Boltzmann equation to account for the non-equilibrium effects induced by laser excitation.[42] In a next step, the PIC model could describe the space charge correction to the external electric field[23,30] above the surface.

To summarize, we investigated electron emission from a negatively biased metallic cathode induced by an ultrashort laser pulse. The electrons within the sample were modeled by Boltzmann scattering integrals, whereas the emitted electrons were studied by a Particle-In-Cell model. It was found that the electron energy distribution has a significant influence on the emission process: The non-equilibrium distribution of the electrons results in a substantial increase in electron emission, compared to its thermal counterpart. Moreover, the accumulated charge above the target alters the potential barrier near the surface and suppresses further emission by electron tunneling. In the limiting case, the electric field induced by the emitted charge compensates the external electric field and saturation is observed. In conclusion, a hybrid model combining a kinetic approach for the non-equilibrium effects within the sample with a space charge-model is indispensable for the description of ultrashort laser-induced electron emission. In future work, a consistent treatment of the near-surface region will be inserted in the model.

The authors would like to thank the FistUA computing facilities at the University of Antwerp, and the Deutsche Forschungsgemeinschaft (DFG, Grant No. RE 1141/15) for financial support.

[1]B. J. Siwick, J. R. Dwyer, R. E. Jordan, and R. J. D. Miller, Science **302**, 1382 (2003).
[2]A. H. Zewail, Annu. Rev. Phys. Chem. **57**, 65 (2006).
[3]H. Ihee, V. A. Lobastov, U. M. Gomez, B. M. Goodson, R. Srinivasan, C. Y. Ruan, and A. H. Zewail, Science **291**, 458 (2001).
[4]H. Niikura, F. Légaré, R. Hasbani, A. D. Bandrauk, M. Y. Ivanov, D. M. Villeneuve, and P. B. Corkum, Nature **417**, 917 (2002).
[5]M. Merano, S. Sonderegger, A. Crottini, S. Collin, P. Renucci, E. Pelucchi, A. Malko, M. H. Baier, E. Kapon, B. Deveaud, and J.-D. Ganière, Nature **438**, 479 (2005).

[6]P. Hommelhoff, C. Kealhofer, and M. A. Kasevich, Phys. Rev. Lett. **97**, 247402 (2006).
[7]P. Hommelhoff, Y. Sortais, A. Aghajani-Talesh, and M. A. Kasevich, Phys. Rev. Lett. **96**, 077401 (2006).
[8]K. L. Jensen and E. J. Montgomery, J. Comput. Theor. Nanosci. **6**, 1754 (2009).
[9]S. Grafstrom, J. Appl. Phys. **91**, 1717 (2002).
[10]A. Gloskovskii, D. Valdaitsev, S. A. Nepijko, G. Schönhense, and B. Rethfeld, Surf. Sci. **601**, 4706 (2007).
[11]N. M. Bulgakova, A. V. Bulgakov, and O. F. Bobrenok, Phys. Rev. E **62**, 5624 (2000).
[12]N. M. Bulgakova, J. Laser Micro/Nanoeng. **2**, 76 (2007).
[13]T. Balasubramani and S. H. Jeong, J. Phys.: Conf. Ser. **59**, 595 (2007).
[14]R. Stoian, A. Rosenfeld, D. Ashkenasi, I. Hertel, N. Bulgakova, and E. Campbell, Phys. Rev. Lett. **88**, 097603 (2002).
[15]E. Gamaly, A. Rode, V. Tikhonchuk, and B. Lutherdavies, Appl. Surf. Sci. **197–198**, 699 (2002).
[16]R. H. Fowler and L. Nordheim, Proc. R. Soc. London **119**, 173 (1928).
[17]L. DuBridge, Phys. Rev. **43**, 727 (1933).
[18]W. Spicer, Phys. Rev. **112**, 114 (1958).
[19]S. I. Anisimov, Phys. Lett. A **55**, 449 (1976).
[20]J. P. Girardeau-Montaut and C. Girardeau-Montaut, Phys. Rev. B **51**, 13560 (1995).
[21]G. Ferrini, F. Banfi, C. Giannetti, and F. Parmigiani, Nucl. Instrum. Methods Phys. Res. A **601**, 123 (2009).
[22]P. Dombi, F. Krausz, and G. Farkas, J. Mod. Opt. **53**, 163 (2006).
[23]W. Wendelen, B. Y. Mueller, D. Autrique, B. Rethfeld, and A. Bogaerts, J. Appl. Phys. **111**, 113110 (2012).
[24]E. Chulkov, V. Silkin, and P. Echenique, Surf. Sci. **391**, L1217 (1997).
[25]M. Faraggi, M. Gravielle, and V. Silkin, Phys. Rev. A **73**, 032901 (2006).
[26]M. Faraggi, M. Gravielle, and D. Mitnik, Phys. Rev. A **76**, 012903 (2007).
[27]R. K. Li, H. To, G. Andonian, J. Feng, A. Polyakov, C. M. Scoby, K. Thompson, W. Wan, H. A. Padmore, and P. Musumeci, Phys. Rev. Lett. **110**, 074801 (2013).
[28]D. M. Riffe, X. Y. Wang, M. C. Downer, D. L. Fisher, T. Tajima, J. L. Erskine, and R. M. More, J. Opt. Soc. Am. B **10**, 1424 (1993).
[29]E. Nelson and J. Petillo, IEEE Trans. Plasma Sci. **32**, 1223 (2004).
[30]W. Wendelen, D. Autrique, and A. Bogaerts, Appl. Phys. Lett. **96**, 051121 (2010).
[31]A. Rokhlenko, K. L. Jensen, and J. L. Lebowitz, J. Appl. Phys. **107**, 014904 (2010).
[32]H. Yamamoto, H. Hamabe, S. Sone, S. Yamaguchi, and M. R. Asakawa, International Journal of Optics **2011**, 714265 (2011).
[33]S. Amoruso, M. Armenante, R. Bruzzese, N. Spinelli, R. Velotta, and X. Wang, Appl. Phys. Lett. **75**, 7 (1999).
[34]B. Cho, T. Ichimura, R. Shimizu, and C. Oshima, Phys. Rev. Lett. **92**, 246103 (2004).
[35]C. Ropers, T. Elsaesser, G. Cerullo, M. Zavelani-Rossi, and C. Lienau, New J. Phys. **9**, 397 (2007).
[36]B. Barwick, C. Corder, J. Strohaber, N. Chandler-Smith, C. Uiterwaal, and H. Batelaan, New J. Phys. **9**, 142 (2007).
[37]R. Ganter, R. Bakker, C. Gough, S. Leemann, M. Paraliev, M. Pedrozzi, F. Le Pimpec, V. Schlott, L. Rivkin, and A. Wrulich, Phys. Rev. Lett. **100**, 064801 (2008).
[38]S. Tsujino, F. Le Pimpec, J. Raabe, M. Buess, M. Dehler, E. Kirk, J. Gobrecht, and A. Wrulich, Appl. Phys. Lett. **94**, 093508 (2009).
[39]H. Yanagisawa, M. Hengsberger, D. Leuenberger, M. Klöckner, C. Hafner, T. Greber, and J. Osterwalder, Phys. Rev. Lett. **107**, 087601 (2011).
[40]R. Gomer, *Field Emission and Field Ionization*, edited by F. V. Hunt (Harvard University Press, Cambridge, Massachusets, 1961), p. 195.
[41]L. Wu and L. K. Ang, Phys. Rev. B **78**, 224112 (2008).
[42]L. K. Ang and M. Pant, Phys. Plasmas **20**, 056705 (2013).
[43]B. Rethfeld, A. Kaiser, M. Vicanek, and G. Simon, Phys. Rev. B **65**, 214303 (2002).
[44]B. Y. Mueller and B. Rethfeld, Phys. Rev. B **87**, 035139 (2013).
[45]C. K. Birdsall and A. B. Langdon, *Plasma Physics and Controlled Fusion* (Adam Hilger, Bristol, 1992), Vol. 34, p. 479.
[46]F. Le Pimpec, C. Milne, C. Hauri, and F. Ardana-Lamas, Appl. Phys. A **112**, 647 (2013).
[47]B. Y. Mueller, T. Roth, M. Cinchetti, M. Aeschlimann, and B. Rethfeld, New J. Phys. **13**, 123010 (2011).
[48]B. Y. Mueller, A. Baral, S. Vollmar, M. Cinchetti, M. Aeschlimann, H. C. Schneider, and B. Rethfeld, Phys. Rev. Lett. **111**, 167204 (2013).